

Anyonic braiding phases in a rotating strongly correlated photon gas

R. O. Umucalılar* and I. Carusotto

INO-CNR BEC Center and Dipartimento di Fisica, Università di Trento, I-38123 Povo, Italy

(Dated: October 12, 2012)

We present a theoretical study of a rotating trapped photon gas where a Laguerre-Gauss laser pump with a non-zero orbital angular momentum is used to inject rotating photons into a cavity with strong optical nonlinearity. The Laughlin-like few-photon eigenstates appear as sharp resonances in the transmission spectra. Using additional localized repulsive potentials, quasi-holes can be created in the quantum Hall liquid of photons and then braided around in space: an unambiguous signature of the many-body Berry phase under exchange of two quasi-holes is observed as a spectral shift of the corresponding transmission resonance.

Quasi-particles with fractional statistics are among the most fascinating discoveries of contemporary condensed-matter physics [1, 2] and are raising an ever growing excitement in view of topological quantum computation applications [3]. In the last decade, nonlinear optical systems are emerging as an outstanding new platform to study many-body physics in fluids of light [4]: superfluid hydrodynamic effects have been investigated with unprecedented detail [5] and strongly correlated states like Mott insulator [6] or Tonks-Girardeau gases [7, 8] are under active experimental study. In the present work, we present a theoretical study of a rotating trapped photon gas: A Laguerre-Gauss laser pump with a non-zero orbital angular momentum is used to inject rotating photons into a cavity with strong optical nonlinearity, and the Laughlin-like few-photon eigenstates [9, 10] appear as sharp resonances in the transmission spectra. Additional localized repulsive potentials are used to create quasi-holes in the quantum Hall liquid of photons and then to braid them around: an unambiguous signature of the many-body Berry phase [11] under exchange of two quasi-holes is observed as a spectral shift of the corresponding transmission resonance.

The close analogy between the Coriolis force in a rotating reference frame and the Lorentz force on a charged particle in a magnetic field is well-known from textbook mechanics and in recent years has been widely exploited to study the analogs of the Meissner effect in superfluids of neutral atoms and the appearance of quantized vortices at higher rotation speeds [12]. Extension of this research into the quantum Hall regime is actively in progress using synthetic gauge fields stemming from the Berry phase accumulated by an optically dressed atom while adiabatically moving in space [13].

In the photonic context, even though optical vortices in nonlinear optical media have received a great attention since the earliest works in fluids of light [4], the interplay of the orbital angular momentum of light with strong photon-photon interactions at the single quantum level has not been investigated yet. Here, we explore this physics in a single cavity geometry: resonant

transmission peaks are associated [8, 14] to strongly correlated few-photon states having an excellent overlap with Laughlin states [15]. Even more remarkably, the many-body Berry phase connected to the braiding of one quasi-hole around another [16] turns out to be directly observable as a spectral shift of a resonant transmission peak, hopefully without the interpretation difficulties arising from competing effects in electron gas experiments based on interferometry [1, 17]. Furthermore, in contrast to previous studies of quantum Hall states of photons [14, 18, 19], our proposal does not require sophisticated photonic configurations and the synthetic magnetic field is generated by the non-zero angular momentum of the pump.

The physical system we are considering is a single optical cavity with cylindrical symmetry consisting of a pair of spherical mirrors and containing a slab of nonlinear medium as sketched in Fig. 1(a). Transverse modes with a given longitudinal mode number \mathcal{N}_z along the cavity axis $\hat{\mathbf{z}}$ can be described as the eigenstates of an isotropic two-dimensional harmonic oscillator of frequency $\omega = \sqrt{2c^2/RL}$, L being the central distance between the two mirrors and R their radius of curvature. Neglecting for simplicity light polarization effects and restricting ourselves to a single longitudinal mode, the many-body dynamics of cavity photons can be described in second quantization terms via the field Hamiltonian [4]

$$\begin{aligned} \mathcal{H} = \int d^2\mathbf{r} \left\{ \frac{\hbar^2}{2m_{ph}} \nabla \hat{\Psi}^\dagger(\mathbf{r}) \nabla \hat{\Psi}(\mathbf{r}) + \right. \\ \left. + \left[\hbar\omega_c + \frac{m_{ph}\omega^2 r^2}{2} + V_{qh}(\mathbf{r}, t) \right] \hat{\Psi}^\dagger(\mathbf{r}) \hat{\Psi}(\mathbf{r}) + \right. \\ \left. + \frac{\hbar g_{nl}}{2} \hat{\Psi}^\dagger(\mathbf{r}) \hat{\Psi}^\dagger(\mathbf{r}) \hat{\Psi}(\mathbf{r}) \hat{\Psi}(\mathbf{r}) + \right. \\ \left. \hbar F(\mathbf{r}, t) \hat{\Psi}^\dagger(\mathbf{r}) + \hbar F^*(\mathbf{r}, t) \hat{\Psi}(\mathbf{r}) \right\}. \quad (1) \end{aligned}$$

Photons in the given longitudinal mode are described by the two-dimensional quantum field $\hat{\Psi}(\mathbf{r})$ satisfying two-dimensional bosonic commutation rules $[\hat{\Psi}(\mathbf{r}), \hat{\Psi}^\dagger(\mathbf{r}')] = \delta^{(2)}(\mathbf{r} - \mathbf{r}')$. The confinement between the two mirrors is responsible for the finite photon rest frequency $\omega_c = c\pi\mathcal{N}_z/L$ and its mass $m_{ph} = \hbar\omega_c/c^2$ and the mirror curvature provides the harmonic trapping potential of frequency ω . Of course, this same Hamiltonian can be used

*Electronic address: onur@science.unitn.it

to describe a variety of other configurations, e.g. solid-state planar microcavities with a suitable lateral patterning [20, 21], or even hybrid set-ups with a spherical fiber-tip mirror facing a planar DBR mirror [22]. The additional potential $V_{qh}(\mathbf{r}, t)$ will be taken as a sum of repulsive delta-shaped potentials centered at time-dependent positions $\mathbf{r}_i^{(L)}(t)$, $V_{qh}(\mathbf{r}, t) = \sum_{i=1}^{N_{qh}} V_0 \delta^{(2)}(\mathbf{r} - \mathbf{r}_i^{(L)}(t))$ and will serve to create the N_{qh} quasi-holes in the fluid: thanks to the fast modulation speed of optical beams, all-optical techniques as the ones demonstrated in [23, 24] can be used to generate these time-dependent potentials.

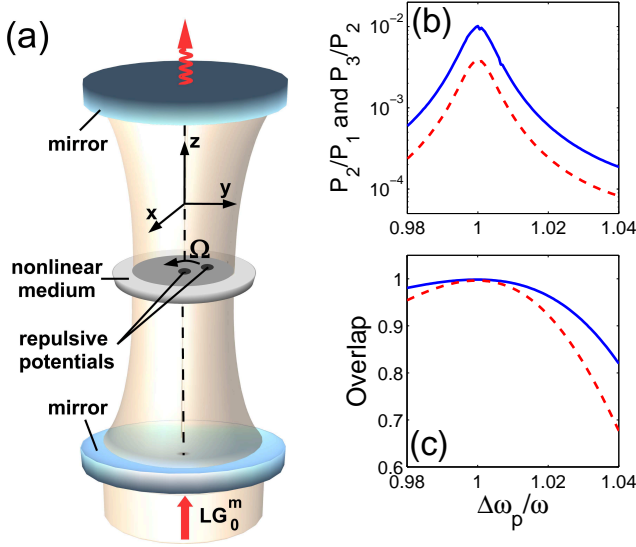


FIG. 1: (a) Sketch of the experimental setup. (b) Steady-state relative probability of two-particle excitation P_2/P_1 (solid line) and of three-particle excitation P_3/P_2 (dashed line) in the absence of repulsive potentials under a monochromatic Laguerre-Gauss pump LG_0^1 and LG_0^2 , respectively. (c) Overlap of the two- (solid line) and three-photon (dashed line) amplitudes with the corresponding Laughlin wave function. System parameters: $\Omega/\omega = 1$, $g_{nl}/\ell^2\omega = 4$, $\gamma/\omega = 0.01$, $\ell F/\gamma = 0.1$. The three-body calculation is performed within the LLL approximation.

The strength of photon-photon interactions is quantified by the interaction coefficient g_{nl} proportional to the $\chi^{(3)}$ nonlinearity of the medium embedded in the cavity: in order to maximize its value, most promising choices may be a cloud of optically dressed atoms in a Rydberg EIT configuration [25] or, in a solid-state context, a quantum well layer with an excitonic optical transition strongly coupled to the cavity photon [4, 22, 26].

Injection of photons into the cavity by a coherent pump laser is described by the last line of the Hamiltonian, the spatio-temporal profile of the laser being fixed by the function $F(\mathbf{r}, t)$: in the following, we shall restrict our attention to the case of monochromatic pumps at frequency $\omega_p^{(L)}$ with the spatial profile of a Laguerre-Gauss beam LG_n^m with orbital angular momentum m centered on the cavity axis. Photon losses at a rate γ are included as Lindblad terms in the master equation for the density

matrix [27].

In the following, it will be useful to describe the system from a reference frame rotating at angular frequency Ω around $\hat{\mathbf{z}}$. To this purpose, one can either add to the Hamiltonian (1) a single term proportional to the total angular momentum L_z along the rotation axis $\hat{\mathbf{z}}$, $\mathcal{H}_\Omega = \mathcal{H} - \Omega L_z$, or include the centrifugal force as a reduction of the effective trapping frequency $\omega^2 \rightarrow \omega^2 - \Omega^2$ and then separately account for the Coriolis force in terms of a vector potential $\mathbf{A}(\mathbf{r}) = m_{ph} \Omega \hat{\mathbf{z}} \times \mathbf{r}$ minimally coupled to the photon momentum as $-i\hbar\nabla \rightarrow -i\hbar\nabla - \mathbf{A}(\mathbf{r})$. While the former formulation is most convenient in calculations, this latter one emphasizes the close analogy with the dynamics of a charged particle in a magnetic field. Of course, in the rotating reference frame, the positions \mathbf{r}_i of the delta potentials have to be accordingly rotated back by an angle Ωt with respect to the laboratory frame ones $\mathbf{r}_i^{(L)}$, and the pump frequency is shifted to $\omega_p = \omega_p^{(L)} - m\Omega$. In the following, pump frequencies will be measured from the photon rest frequency as $\Delta\omega_p = \omega_p - \omega_c$.

Based on the Hamiltonian (1), we now discuss how it is possible to generate a Laughlin state of photons in the cavity without repulsive delta potentials ($V_0 = 0$). We start by considering the isolated system Hamiltonian \mathcal{H}_Ω in the frame rotating at Ω in the absence of driving ($F = 0$) and losses ($\gamma = 0$). When $\Omega \rightarrow \omega$, this Hamiltonian is seen to be formally identical to the one describing the fractional quantum Hall (FQH) physics of interacting electrons in a magnetic field, if one replaces the Coulomb interactions with the present contact interactions. In particular, the N -particle ground state of \mathcal{H}_Ω is well represented by the $\nu = 1/2$ bosonic Laughlin wave function

$$\Psi_{FQH}(z_1, \dots, z_N) = \prod_{j < k} (z_j - z_k)^2 e^{-\sum_{i=1}^N |z_i|^2/2}, \quad (2)$$

where $z_j = (x_j + iy_j)/\ell$ are the complex particle coordinates in units of the oscillator length $\ell = \sqrt{\hbar/m_{ph}\omega}$ [9, 15]. This wave function is composed of lowest Landau level (LLL) wave functions, has a total angular momentum $M = \hbar N(N-1)$ and is separated from the excited states by an energy gap approximately given by $g_{nl}/4\pi\ell^2$ in the low g_{nl} limit where the LLL approximation is valid (cfr. Sec. I of the Supplemental Material).

Inspired from our previous work [14], we propose to create such a Laughlin state optically by exploiting the driven-dissipative nature of the photonic system. A Monte Carlo wave function calculation of the steady-state density matrix [14, 28] shows that the cavity transmission under continuous-wave pumping and losses displays a peculiar dependence on the pump frequency $\Delta\omega_p$: for sufficiently low photon losses, sharp resonance peaks corresponding to the eigenstates of the isolated system appear. An effective choice to excite the Laughlin state is to use a Laguerre-Gauss LG_0^m incident beam with orbital angular momentum $m = N-1$ chosen to match the value

$N-1$ of the angular momentum per particle of the target N -particle Laughlin state. The efficiency of this strategy is illustrated in Fig. 1(b,c) for the $N = 2, 3$ cases.

In panel (b), we show a simulated spectrum of the relative probability P_N/P_{N-1} of having N photons in the cavity as a function of pump frequency $\Delta\omega_p$ in the frame rotating at $\Omega = \omega$. Plotting the ratio P_N/P_{N-1} allows to put in better evidence the role of the N -photon states over the background of lower states: As usual [8], the position of the transmission peak is related to the N -body eigenenergies by the resonance condition $\omega_p = \omega^{(N)}/N = \omega_c + \omega$. For both $N = 2, 3$, the main peaks at $\Delta\omega_p/\omega = 1$ correspond to an N -photon transition from vacuum to the lowest N -particle eigenstate of H_Ω at energy $\hbar\omega^{(N)} = N\hbar(\omega_c + \omega)$ fixed by the zero-point motion in the harmonic potential. This suggests that particles are non-overlapping in this state.

As a check of the Laughlin nature of the state, we can look at the overlap $\mathcal{O}(\Psi_{FQH}, \Phi) = |\langle \Psi_{FQH} | \Phi \rangle|^2 / \langle \Psi_{FQH} | \Psi_{FQH} \rangle \langle \Phi | \Phi \rangle$ between the N -photon amplitude $\Phi(z_1, \dots, z_N) = \text{Tr}[\rho_{ss} \hat{\Psi}(z_1) \dots \hat{\Psi}(z_N)]$ and the target Laughlin wave function Ψ_{FQH} . As we discussed in [14], in the weak driving limit $\ell F/\gamma \ll 1$, the N -photon amplitude gives in fact the many-body wave function of the single N -particle pure state reached by the system and is experimentally accessible from repeated measurements of the field quadratures of the transmitted light. Its dependence on the pump frequency $\Delta\omega_p$ is shown in Fig. 1(c): as expected, the maximum overlap is obtained at $\Delta\omega_p/\omega = 1$; its peak value larger than 99.5% confirms that the generated state is basically the N -particle Laughlin state. As angular momentum of the rotating gas is continuously replenished by the pump beam, the photon system is much less sensitive to trap anisotropies than atomic clouds: as a result, the overlap with the Laughlin state is still $\approx 97\%$ for trap anisotropies as large as $(\omega_x - \omega_y)/(\omega_x + \omega_y) = 0.02$.

We can now turn to the generation of quasi-holes in the quantum Hall liquid. This can be done by adding localized repulsive potentials to pierce holes in the photon gas. As indicated in Eq. (1), their strength is denoted by V_o . Their position $\mathbf{r}_i^{(L)}(t)$ is assumed to be rotating at an angular frequency Ω in the laboratory frame, in order to be stationary at \mathbf{r}_i in the frame rotating at Ω . In the absence of pumping and losses, and for $\Omega \rightarrow \omega$, the ground state of the one-quasi-hole Hamiltonian \mathcal{H}_Ω° is successfully represented by the single quasi-hole wave function [2, 9, 15].

$$\Psi_o(z_1, \dots, z_N) = \prod_i (z_i - z_o) \Psi_{FQH}(z_1, \dots, z_N), \quad (3)$$

where $z_o = r_o e^{i\theta_o}/\ell$ is the complex coordinate of the quasi-hole (cfr. Sec. I of the Supplemental Material). Another quasi-hole sitting, e.g., at the center of the trap $z_{oo} = 0$ can be included via a second delta-function potential in the two quasi-hole Hamiltonian $\mathcal{H}_\Omega^{\circ\circ}$. Again, in the $\Omega \rightarrow \omega$ limit, the ground state wave function can be

written in the simple form

$$\Psi_{oo}(z_1, \dots, z_N) = \prod_i (z_i - z_o) z_i \Psi_{FQH}(z_1, \dots, z_N). \quad (4)$$

The crucial point of our proposal is to relate the braiding phase observed in the reference frame rotating at the trap frequency ω to the time-independent energy spectrum in the frame rotating at slightly lower $\Omega = \omega - \delta\Omega$. In the frame rotating at ω , the quasi-hole at z_o is in fact slowly rotating at frequency $\delta\Omega$ in the backwards direction: provided $\delta\Omega$ is small enough, this process is equivalent to adiabatically looping the quasi-hole at z_o along the circle of radius r_o following the position of the localized potential. As a result, after a rotation period $T = 2\pi/\delta\Omega$, the quasi-hole will return to its original position [11], with the single (double) quasi-hole wave function Ψ_o (Ψ_{oo}) having acquired a Berry phase ϕ_B° ($\phi_B^{\circ\circ}$) in addition to the trivial dynamical phase $E_\omega^\circ T$ ($E_\omega^{\circ\circ} T$).

When observed from the reference frame rotating at Ω where the localized potentials are fixed in space, the time evolution reduces for any t to the phase $E_\Omega^{\circ,\circ\circ} t$. At time $t = T$ when a rotation is complete, the wave functions in the two frames have to coincide again, which establishes a relation between the energy difference $\Delta E^{\circ,\circ\circ} = E_\omega^{\circ,\circ\circ} - E_\Omega^{\circ,\circ\circ}$ and the many-body Berry phases $\phi_B^{\circ,\circ\circ}$,

$$\phi_B^{\circ,\circ\circ} = 2\pi \frac{\Delta E^{\circ,\circ\circ}}{\hbar \delta\Omega} \pmod{2\pi}. \quad (5)$$

This relation holds for both quasi-hole states in a quantum Hall liquid, as well as in a non-interacting system (cfr. Sec. III of the Supplemental Material). As it relates the many-body Berry phase to spectroscopically observable quantities such as the energies, it will be the basis of the measurement scheme we are now going to illustrate.

As a first step, we wish to numerically confirm Eq. (5) for the isolated system. To this purpose, we look for the ground state wave functions in the rotating frame at Ω where the quasi-holes are fixed in space and the Hamiltonians \mathcal{H}_Ω° and $\mathcal{H}_\Omega^{\circ\circ}$ are time-independent. Their overlap with the analytic wave-functions (3) and (4) for $\Omega/\omega = 0.99$ is shown in Fig. 2(a) as a function of the position r_o of the exterior quasi-hole. In the lower panel, we show the value of the braiding phase $\phi_{Br} = \phi_B^\circ - \phi_B^{\circ\circ}$: as introduced in [16], this is the difference between the many-body Berry phases acquired by the ground state wave functions in the presence of single and double delta-function potentials. In this panel, the value of ϕ_{Br} extracted via Eq. (5) from experimentally accessible quantities is compared with the result of a direct calculation of the Berry phases from the analytical wave functions (3) and (4) (cfr. Sec. II of the Supplemental Material). The agreement is excellent up to a radius $r_o \approx \ell$, i.e. when the quasi-hole potential starts exiting the cloud: at this point, the repulsive delta potential is no longer able to sustain the quasi-hole state and the overlap shown in panel (a) suddenly drops.

The optical generation of the quasi-hole states is illustrated in Fig. 3: a monochromatic Laguerre-Gauss

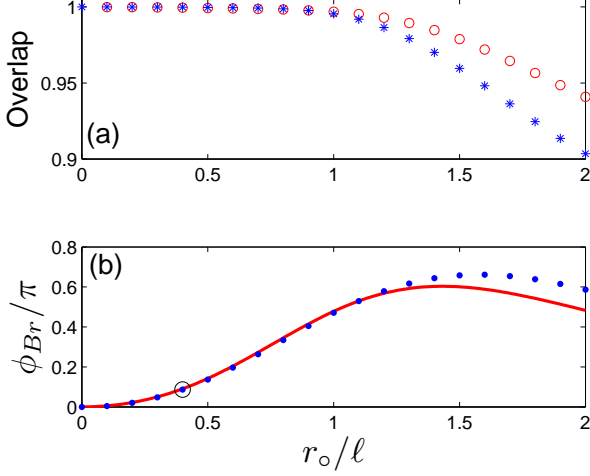


FIG. 2: (a) Stars * (circles o) show the overlap of the $N = 2$ lowest energy eigenstate of \mathcal{H}_Ω° ($\mathcal{H}_\Omega^{\circ\circ}$) with the one (two) quasi-hole wave function Ψ_\circ ($\Psi_{\circ\circ}$) as a function of the position r_o of the exterior quasi-hole. (b) Estimation (•) of the braiding phase calculated via Eq. (5) compared with the analytical result from the quasi-hole wave functions Ψ_\circ , $\Psi_{\circ\circ}$ (solid line). System parameters $g_{nl}/\ell^2\omega = 4$, $\Omega/\omega = 0.99$ and $V_o/\ell^2\hbar\omega = 100$.

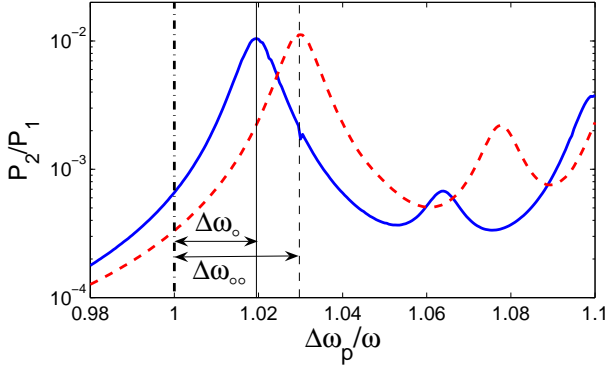


FIG. 3: Steady-state relative probability P_2/P_1 of two-particle excitation for \mathcal{H}_Ω° with a Laguerre-Gauss LG_0^2 pump (solid line), and for $\mathcal{H}_\Omega^{\circ\circ}$ and an LG_0^3 pump (dashed line). Vertical solid (dashed) lines correspond to half the eigenenergies of the isolated system. System and pump parameters as in Fig. 1, with $\Omega/\omega = 0.99$, $r_o = 0.4$ and $V_o/\ell^2\hbar\omega = 100$.

beam is shined on the cavity in the presence of the repulsive potentials rotating at a frequency $\Omega/\omega = 0.99$. An efficient choice for the orbital angular momentum of the pump is to use the closest integer to the angular momentum per particle of the target state. The steady-state density matrix is numerically calculated via Monte Carlo wave function technique in the frame rotating at Ω where the Hamiltonian is time-independent. The different curves in the figure show the spectrum of P_2/P_1 as a function of pump frequency $\Delta\omega_p$: the solid (dashed) curve refers to the one (two) quasi-hole Hamiltonian \mathcal{H}_Ω° ($\mathcal{H}_\Omega^{\circ\circ}$) including one (two) localized repulsive potential. The most relevant features are the lowest frequency peaks at $\Delta\omega_p/\omega = 1.0195$ on the solid line and 1.0297 on the dashed one: their identification with quasi-hole states is confirmed by the excellent overlap $\approx 99\%$ of the two-photon amplitude with the analytical wave functions in (3) and (4). Remembering that these two-photon peaks are located at half the energy $E_\Omega^{\circ\circ}$ of the two-photon eigenstate, it is then straightforward to extract via (5) the value of the many-body Berry phase when one quasi-hole at r_o is braided around another one located at the center of the trap: as one can see from the small circle in Fig. 2(b), the accuracy of this simulated measurement is excellent. An analogous calculation of the position of three-photon peaks (performed within the LLL approximation) suggests the efficiency of the measurement protocol also for states with larger number of particles where the theory of the fractional quantum Hall effect predicts a constant braiding phase of π (cfr. Sec. IV of the Supplementary Material) [2, 10].

In conclusion, we have proposed and characterized an all-optical scheme to generate and manipulate quantum Hall liquids of strongly interacting photons in a nonlinear optical cavity. Quasi-holes in the fluid can be pierced and braided with repulsive potentials and the corresponding many-body Berry phase can be detected from the spectral shifts of the resonant transmission peaks. Extension of this work to more complex configurations involving e.g. light polarization degrees of freedom may open the way to observe anyonic excitations with non-Abelian statistics.

We are grateful to A. Imamoglu, R. Santachiara and T. Volz for stimulating discussions. The authors acknowledge financial support from ERC through the QGBE grant.

-
- [1] A. Stern, *Ann. Phys.* **323**, 204 (2008).
 - [2] D. Yoshioka, *The Quantum Hall Effect* (Springer-Verlag, Berlin, 2002).
 - [3] C. Nayak, S. H. Simon, A. Stern, M. Freedman, and S. Das Sarma *Rev. Mod. Phys.* **80**, 1083 (2008).
 - [4] I. Carusotto and C. Ciuti, *Rev. Mod. Phys.* (to appear), preprint arXiv:1205.6500.
 - [5] A. Amo *et al.*, *Nature Phys.* **5**, 805 (2009).
 - [6] M. J. Hartmann, F. G. S. L. Brandão, M. B. Plenio, *Laser Photonics Rev.* **2**, 527 (2008).
 - [7] D. E. Chang *et al.*, *Nature Phys.* **4**, 884 (2008).
 - [8] I. Carusotto *et al.*, *Phys. Rev. Lett.* **103**, 033601 (2009).
 - [9] B. Paredes, P. Fedichev, J. I. Cirac, and P. Zoller, *Phys. Rev. Lett.* **87**, 010402 (2001).
 - [10] B. Juliá-Díaz, T. Grass, N. Barberán, and M. Lewenstein, *New J. Phys.* **14**, 055003 (2012).
 - [11] A. Shapere and F. Wilczek, eds., *Geometric Phases In Physics* (World Scientific, Singapore, 1989).

- [12] A. L. Fetter, Rev. Mod. Phys. **81**, 647 (2009).
- [13] J. Dalibard, F. Gerbier, G. Juzeliūnas, and P. Öhberg, Rev. Mod. Phys. **83**, 1523 (2011).
- [14] R. O. Umucalılar and I. Carusotto, Phys. Rev. Lett. **108**, 206809 (2012).
- [15] R. B. Laughlin, Phys. Rev. Lett. **50**, 1395 (1983).
- [16] D. Arovas, J. R. Schrieffer, and F. Wilczek, Phys. Rev. Lett. **53**, 722 (1984).
- [17] F. E. Camino, W. Zhou, and V. J. Goldman, Phys. Rev. B **72**, 075342 (2005).
- [18] J. Cho, D. G. Angelakis, and S. Bose, Phys. Rev. Lett. **101**, 246809 (2008).
- [19] A. L. C. Hayward, A. M. Martin, and A. D. Greentree, Phys. Rev. Lett. **108**, 223602 (2012).
- [20] D. Lu, J. Ahn, S. Freisem, D. Gazula, and D. G. Deppe, Appl. Phys. Lett. **87**, 163105 (2005).
- [21] O. El Daif *et al.*, Appl. Phys. Lett. **88**, 061105 (2006).
- [22] B. Besga *et al.*, to be published (2012).
- [23] A. Amo *et al.*, Phys. Rev. B **82**, 081301 (2010).
- [24] A. Hayat *et al.*, Phys. Rev. Lett. **109**, 033605 (2012).
- [25] T. Peyronel *et al.*, Nature **488**, 57 (2012).
- [26] P. Cristofolini *et al.*, Science **336**, 704 (2012).
- [27] D. F. Walls and G. J. Milburn, *Quantum Optics*, 2nd edition, (Springer-Verlag, Berlin, 2008).
- [28] K. Mølmer, Y. Castin, and J. Dalibard, J. Opt. Soc. Am. B **10**, 524 (1993).

Supplemental Material

I. DEPENDENCE OF EIGENSTATES AND EIGENERGIES ON THE RELATIVE ANGULAR FREQUENCY $\delta\Omega$

In this section we justify the adiabatic following of the ground state when the quasi-hole potential is braided around in space.

Let us start from the Hamiltonian \mathcal{H}_Ω with no repulsive localized potentials. The energies of the eigenstates of \mathcal{H}_Ω are plotted in Fig. 1(a) as a function of $\delta\Omega$. For $\delta\Omega \rightarrow 0$, we have a sequence of massively degenerate states: the lowest manifold corresponds to wave functions obtained as the product of a Laughlin state Ψ_{FQH} , as defined in Eq. (3) of the main text, times any polynomial symmetric under $z_1 \leftrightarrow z_2$ and is separated from the higher manifold by a gap mostly determined by the interaction strength g_{nl} . Within the lowest Landau Level (LLL) approximation valid for small $g_{nl}/\ell^2 \ll \hbar\omega$, the gap is proportional to g_{nl} and close to the integral $g_{nl} \int |\psi_0(\mathbf{r})|^4 d^2\mathbf{r}/2 = g_{nl}/4\pi\ell^2$, ψ_0 being the harmonic oscillator ground state wave function. For finite $\delta\Omega$, the states of the first manifold are split according to their total angular momentum. The non-degenerate ground state has the lowest angular momentum $\hbar N(N-1)$ and is given by the Laughlin state Ψ_{FQH} . The first excited state has one more unit of angular momentum and is separated from the ground state by $\hbar\delta\Omega$.

We have then performed a numerical diagonalization of the Hamiltonian $\mathcal{H}_\Omega^{\circ,\circ}$ in the presence of one and two localized repulsive potentials piercing quasi-holes through the quantum Hall liquid. The result for the two quasi-hole case is shown in Fig. 1(b): for small but non-zero $\delta\Omega$, the ground state is separated from the first excited state by a small amount close to $\hbar\delta\Omega$. The next manifold lies higher in energy by an amount determined by g_{nl} . States involving non-lowest-Landau-level components are found at even higher energies of the order of $\hbar\omega$. The quasi-hole nature of the ground state is numerically confirmed by a calculation of its overlap with the two quasi-hole wave function, as given by Eq. (4) of the main text. The higher states of the manifold correspond to wave functions obtained by multiplying this two quasi-hole wave function by arbitrary symmetric polynomials.

The fact that the two quasi-hole state is the ground state even for non-zero values of $\delta\Omega$ confirms that holes are indeed braided around the quantum Hall fluid without creating excitations provided braiding is performed slowly enough. As we have seen in the main text, the overlap with the quasi-hole wave function suddenly drops at some value of the quasi-hole position r_o . An analogous phenomenon is visible here as a function of angular frequency $\delta\Omega$ in Fig. 1(c): overlap suddenly drops at the first avoided crossing point between the ground state and a lower angular momentum state from the higher manifold.

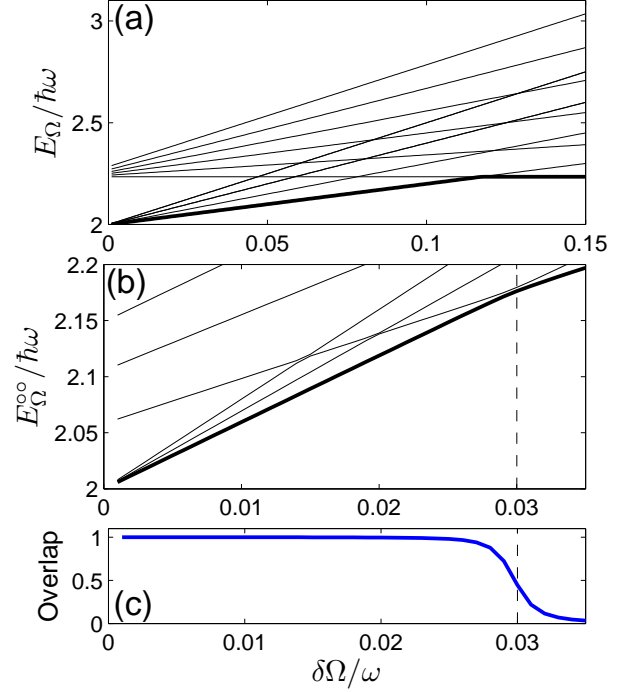


FIG. 1: (a) Energy of the lowest $N = 2$ particle eigenstates of \mathcal{H}_Ω as a function of relative rotation frequency $\delta\Omega = \omega - \Omega$ in the absence of the repulsive quasi-hole potentials. For clarity, only the states of total angular momentum $L_z \leq 5$ are displayed. (b) Energy of the lowest $N = 2$ particle eigenstates of the two quasi-hole Hamiltonian $\mathcal{H}_\Omega^{\circ,\circ}$ as a function of relative rotation frequency $\delta\Omega = \omega - \Omega$. For clarity, only states at low average angular momentum $\langle L_z \rangle < 8$ are displayed. (c) Overlap of the ground state of $\mathcal{H}_\Omega^{\circ,\circ}$ with the analytical two quasi-hole wave function, Eq. (4) of the main text. System parameters: $g_{nl}/\ell^2\omega = 4$, $V_o/\ell^2\hbar\omega = 100$. The exterior quasi-hole is positioned at $r_o = 0.4\ell$.

II. BERRY PHASE FOR ONE AND TWO QUASI-HOLE STATES

Here we prove a simple relation between the expected value of total angular momentum $\langle L_z \rangle$ and the Berry phase ϕ_B acquired by a many-body wave function lying in the LLL, when a quasi-hole is looped along a circle with or without a second quasi-hole sitting at the center of the circle.

The generic form of the N -particle wave function we consider is

$$\Psi(z_1, \dots, z_N; z_o) = \sum_{n_1, \dots, n_N} c_{n_1, \dots, n_N} z_1^{n_1} \dots z_N^{n_N} \times (z_1 - z_o) \dots (z_N - z_o) e^{-\sum_{j=1}^N |z_j|^2/2}, \quad (1)$$

where $z_j = (x_j + iy_j)/\ell$ are the complex particle coordinates, z_o is the quasi-hole coordinate and n_j are non-negative integers. The only assumption we are making is that $\sum_{j=1}^N n_j = A$ is constant, meaning that the part of the wave function shown in the first line is a homogenous multivariate polynomial of degree A . A second quasi-hole term $z_1 \dots z_N$ can be included into this part by letting each n_j increase by 1.

For simplicity, from now on we will omit displaying the exponential factor which is common to all terms in the summation over n_j and use the shorthand notations $\{z\} \equiv z_1, \dots, z_N$, and $\{n\} \equiv n_1, \dots, n_N$. We will also expand the product $(z_1 - z_o) \dots (z_N - z_o)$ as follows $(z_1 - z_o) \dots (z_N - z_o) = \sum_{l=0}^N d_l z_o^l$. Upon these changes, the wave function becomes:

$$\Psi(\{z\}; z_o) \equiv \sum_{\{n\}} c_{\{n\}} z_1^{n_1} \dots z_N^{n_N} \sum_{l=0}^N d_l z_o^l. \quad (2)$$

Let us now calculate ϕ_B for a quasi-hole at $z_o = r_o e^{i\theta_o}/\ell$ with $\bar{r}_o \equiv r_o/\ell$ fixed:

$$\begin{aligned} \phi_B &= -i \int_0^{2\pi} \int d\{z\} d\{z^*\} \Psi^* \partial_{\theta_o} \Psi d\theta_o = \\ &= 2\pi \int d\{z\} d\{z^*\} \sum_{\{n\}, \{n'\}} c_{\{n'\}}^* c_{\{n\}} z_1^{*n'_1} z_1^{n_1} \dots z_N^{*n'_N} z_N^{n_N} \\ &\quad \times \sum_{l=0}^N l |d_l|^2 \bar{r}_o^{2l}, \quad (3) \end{aligned}$$

where $d\{z\} \equiv dz_1 \dots dz_N$ and $\partial_{\theta_o} \equiv \partial/\partial\theta_o$ is the partial derivative with respect to θ_o . Now let us look at the expected value of total angular momentum:

$$\begin{aligned} \langle L_z \rangle &= \int d\{z\} d\{z^*\} \sum_{\{n'\}} c_{\{n'\}}^* z_1^{*n'_1} \dots z_N^{*n'_N} \sum_{l'=0}^N d_{l'}^* z_o^{l'} \\ &\quad \times (-i\hbar)(\partial_{\theta_1} + \dots + \partial_{\theta_N}) \sum_{\{n\}} c_{\{n\}} z_1^{n_1} \dots z_N^{n_N} \sum_{l=0}^N d_l z_o^l \quad (4) \end{aligned}$$

While taking the derivatives ∂_{θ_j} with respect to the angular variables (we have set $z_j = |z_j| e^{i\theta_j}$), we can use the chain rule to isolate the contribution of the $\sum_{l=0}^N d_l z_o^l$ term. In this way, the second line of Eq. (4) becomes

$$\begin{aligned} &\hbar \sum_{\{n\}} c_{\{n\}} (n_1 + \dots + n_N) z_1^{n_1} \dots z_N^{n_N} \sum_{l=0}^N d_l z_o^l \\ &+ \hbar \sum_{\{n\}} c_{\{n\}} z_1^{n_1} \dots z_N^{n_N} \sum_{l=0}^N (N-l) d_l z_o^l. \quad (5) \end{aligned}$$

To get this result one simply has to recall that $d_l = z_1^{s_1} \dots z_N^{s_N}$ with $(s_1 + \dots + s_N) = N-l$. Inserting (5) into Eq. (4), and reordering terms we obtain

$$\begin{aligned} \langle L_z \rangle &= \hbar \sum_{\substack{\{n\}, \{n'\} \\ l, l'}} c_{\{n'\}}^* c_{\{n\}} z_o^{*l'} z_o^l (A + N - l) \\ &\times \int d\{z\} d\{z^*\} z_1^{*n'_1} \dots z_N^{*n'_N} d_{l'}^* z_1^{n_1} \dots z_N^{n_N} d_l. \quad (6) \end{aligned}$$

In order for the integral not to vanish, the total power of conjugated coordinates should match that of unconjugated ones: $A + N - l' = A + N - l$, implying $l' = l$. As a result, one gets

$$\begin{aligned} -2\pi \frac{\langle L_z \rangle}{\hbar} &= -2\pi(A + N) \sum_{\{n\}, \{n'\}} c_{\{n'\}}^* c_{\{n\}} \int d\{z\} d\{z^*\} z_1^{*n'_1} \dots z_N^{*n'_N} \sum_{l=0}^N |d_l|^2 \bar{r}_o^{2l} \\ &+ 2\pi \sum_{\{n\}, \{n'\}} c_{\{n'\}}^* c_{\{n\}} \int d\{z\} d\{z^*\} z_1^{*n'_1} \dots z_N^{*n'_N} \sum_{l=0}^N l |d_l|^2 \bar{r}_o^{2l}. \quad (7) \end{aligned}$$

The first term apart from the factor $-2\pi(A + N)$ is the normalization of the wave function (2), which we take to be 1. The second term is ϕ_B we have found in Eq. (3).

Thus, finally we have

$$\phi_B = -2\pi \frac{\langle L_z \rangle}{\hbar} + 2\pi(A + N). \quad (8)$$

This result can be explicitly checked for the simplest

$N = 1$ and $N = 2$ cases, for which one can analytically calculate ϕ_B and $\langle L_z \rangle$ without much difficulty. Here we do not give the details of the elementary verification and only quote some final results for one and two quasi-hole states.

For the case of $N = 1$, the Berry phase for the single-quasi-hole wave function $\propto (z_1 - z_o)e^{-|z_1|^2/2}$ (here $A = 0$) is

$$\phi_B^{1,\circ} = \frac{2\pi\bar{r}_o^2}{1 + \bar{r}_o^2}, \quad (9)$$

while for the double-quasi-hole wave function $\propto z_1(z_1 - z_o)e^{-|z_1|^2/2}$ (here $A = 1$) it is

$$\phi_B^{1,\circ\circ} = \frac{2\pi\bar{r}_o^2}{2 + \bar{r}_o^2}. \quad (10)$$

For the case of $N = 2$, the Berry phase for the $\nu = 1/2$ Laughlin wave function with a single quasi-hole $\propto (z_1 - z_2)^2(z_1 - z_o)(z_2 - z_o)e^{-(|z_1|^2 + |z_2|^2)/2}$ (here $A = 2$) is

$$\phi_B^{2,\circ} = 2\pi \frac{4\bar{r}_o^2 + 4\bar{r}_o^4}{7 + 4\bar{r}_o^2 + 2\bar{r}_o^4}, \quad (11)$$

while for the double-quasi-hole wave function $\propto (z_1 - z_2)^2 z_1 z_2 (z_1 - z_o)(z_2 - z_o)e^{-(|z_1|^2 + |z_2|^2)/2}$ (here $A = 4$) it is

$$\phi_B^{2,\circ\circ} = 2\pi \frac{18\bar{r}_o^2 + 14\bar{r}_o^4}{60 + 18\bar{r}_o^2 + 7\bar{r}_o^4}. \quad (12)$$

To summarize, the relation given in Eq. (8) provides a direct way to efficiently calculate the Berry phase as soon as the coefficients of each term in the wave function are known [1]: in the last section we shall see an example of its application to states with a larger number of particles N up to 6.

In addition to this, this relation suggests an alternative experimental method to determine the Berry phase for setups where a precise measurement of total angular momentum might be feasible.

III. RESULTS FOR THE NON-INTERACTING SYSTEM

In order to get a deeper understanding of the braiding phase in a quantum Hall liquid, it is interesting to study the structure of the ground state and calculate the Berry phase also in the different case of a non-interacting system with $g_{nl} = 0$.

With no loss of generality, we can start from the $N = 1$ single particle case and calculate the braiding phase ϕ_{Br} in the presence of one and two delta-function potentials using the relation (5) of the main text

$$\phi_B^{\circ,\circ\circ} = 2\pi \frac{\Delta E^{\circ,\circ\circ}}{\hbar \delta \Omega} \pmod{2\pi}. \quad (13)$$

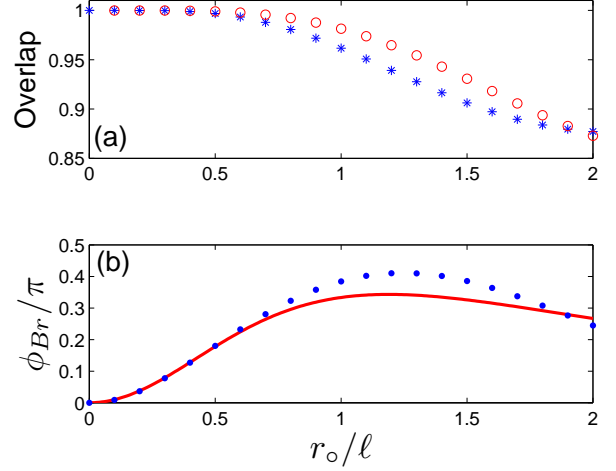


FIG. 2: (a) Stars * (circles o) show the overlap of the lowest energy state wave function of a single particle in the presence of one (two) delta-function potential with the one (two) quasi-hole wave function as a function of the exterior quasi-hole coordinate r_o . System parameters: $\Omega/\omega = 0.99$, $V_o/\ell^2 \hbar \omega = 100$. (b) Braiding phase calculated from Eq. (13) is shown by dots (•); the curve is the analytical result for $\phi_B^{1,\circ} - \phi_B^{1,\circ\circ}$ as given by Eqs. (9) and (10).

The many-body wave function for a larger number N of non-interacting particles is in fact equal to the product of $N = 1$ wave functions, so that both the energy and the braiding phase are just multiplied by a factor N .

The braiding phase as a function of the exterior quasi-hole coordinate r_o is plotted in Fig. 2(a) and compared with the difference $\phi_B^{1,\circ} - \phi_B^{1,\circ\circ}$ calculated from the explicit expressions in Eqs. (9) and (10): once again, the agreement is excellent as long as the repulsive potential is well inside the cloud, $r_o \lesssim 0.5\ell$. This explanation is validated in panel (b) where we show the overlap of the ground state with one and two repulsive potentials with the corresponding analytical forms of the one and two quasi-hole wave functions.

The optical response of the $g_{nl} = 0$ system is a purely linear one: transmission spectra for a Laguerre-Gauss LG_0^1 mode with one unit of angular momentum are shown in Fig. 3 for the single quasi-hole case. As expected, the position of the one photon peak matches the ground state energy of the isolated system. The two-photon peak in the P_2/P_1 spectrum occurs at the same frequency, as expected from the simple fact that the two-photon ground-state energy is twice the single-particle ground-state energy. The Berry phase calculated from the shift $\Delta\omega_o$ of the peak via Eq. (13) is $\approx 0.280\pi$, in good agreement with the analytical prediction $\approx 0.276\pi$ from Eq. (9).

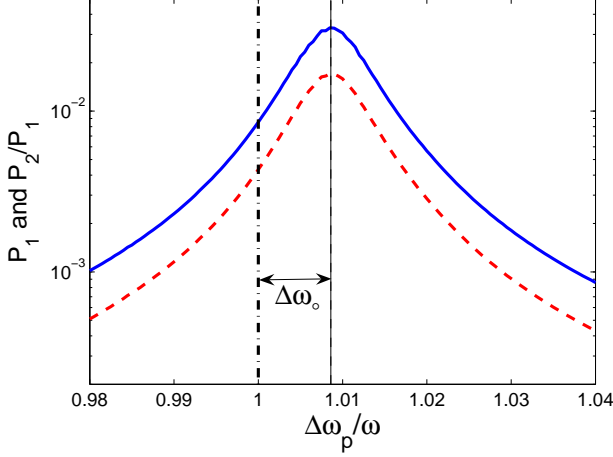


FIG. 3: Steady-state probability of single-particle excitation P_1 (solid line) and the relative probability of two-particle excitation P_2/P_1 (dashed line) in the presence of a single delta potential localized at $r_o = 0.4\ell$ under a monochromatic Laguerre-Gauss LG_0^1 pump. System and pump parameters: $\Omega/\omega = 0.99$, $\gamma/\omega = 0.01$, $\ell F/\gamma = 0.1$.

IV. RESULTS WITH MORE THAN TWO INTERACTING PARTICLES

Some results for larger number of interacting particles are shown in Figs. 4 and 5.

To obtain the braiding phase ϕ_{Br} analytically for $N > 2$ more efficiently, we used the relation (8). In Fig. 4(a), we compare the estimation for ϕ_{Br} obtained for $N = 3, 4$ from the numerical ground state via Eq. (13) with the analytical results from the quasi-hole wave functions. As compared to the $N = 2$ case, it can be seen that the region of good agreement extends further in r_o , which could be expected as the cloud size increases with increasing N .

Panel (b) displays the analytical predictions for ϕ_{Br} as a function of r_o for N up to 6; unfortunately, available computing resources prevent us from directly extending the calculation to higher N values for which more sophisticated Monte Carlo techniques should be used. For increasing N , the position of maximum ϕ_{Br} shifts towards larger r_o and its value gets close to π . This trend is quite different from that of the non-interacting system examined in the previous section, where the braiding phase is simply given by N times the single-particle braiding phase.

For much larger number of particles, the characteristic incompressibility of the quantum Hall liquid is expected to result in a large plateau at $\phi_{Br} = \pi$. In this limit [2, 3], the Berry phase acquired through looping of a quasi-hole can simply be expressed as $2\pi\langle N \rangle$, $\langle N \rangle$ being the average number of particles enclosed by the loop. The effect of an additional quasi-hole inside the loop would be to displace a fraction ν of a particle from an otherwise spatially constant density, leading to an extra braiding

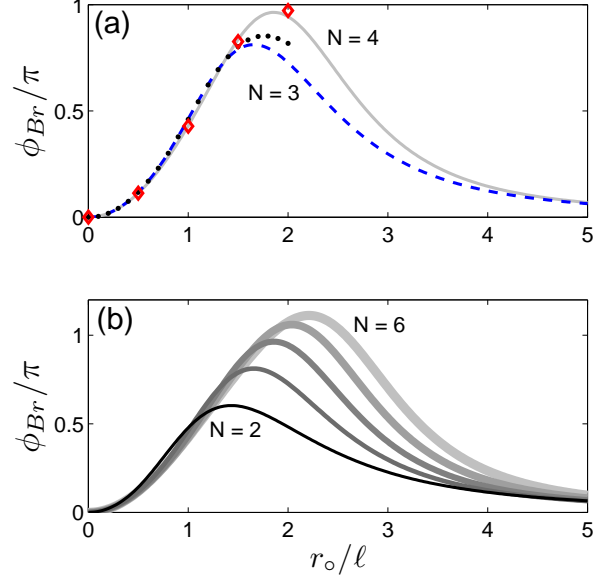


FIG. 4: (a) Braiding phase ϕ_{Br} calculated for $N = 3$ (dashed line) and $N = 4$ (solid line) from the analytical forms of the one and two quasi-hole wave functions, Eqs. (3) and (4) of the main text. Corresponding ϕ_{Br} extracted via Eq. (13) from the numerical ground state of $\mathcal{H}_{\Omega}^{\circ, \circ \circ}$ within the LLL approximation for $N = 3$ (\bullet) and $N = 4$ (\diamond). System parameters: $\Omega/\omega = 0.99$, $g_{nl}/\ell^2\omega = 4$, and $V_o/\ell^2\hbar\omega = 100$. (b) Braiding phase ϕ_{Br} calculated analytically for $N = 2, 3, 4, 5$, and 6 from the analytical forms of the one and two quasi-hole wave functions, Eqs. (3) and (4) of the main text. Line thickness increases with N .

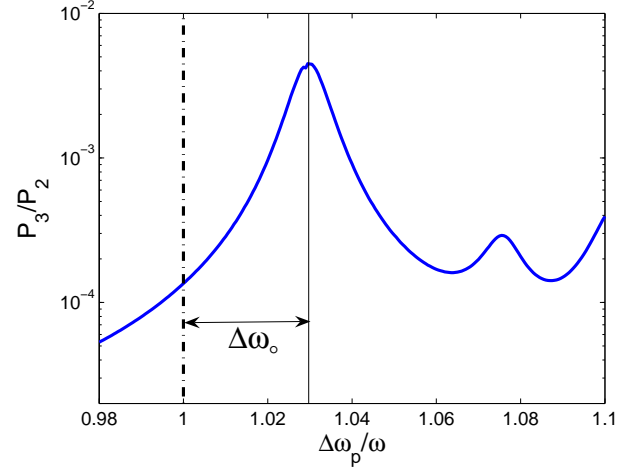


FIG. 5: Steady-state relative probability P_3/P_2 of three-particle excitation in the presence of a single delta potential localized at $r_o = 0.4\ell$ under a monochromatic Laguerre-Gauss LG_0^3 pump. System and pump parameters: $\Omega/\omega = 0.99$, $g_{nl}/\ell^2\omega = 1$, $\gamma/\omega = 0.01$, $\ell F/\gamma = 0.1$.

phase of $2\pi\nu$. For the Laughlin and quasi-hole states considered in the present work, the fraction is $\nu = 1/2$, which results in a braiding phase of π .

In Fig. 5 we simulate the optical excitation of an $N = 3$ particle, one quasi-hole state using a Laguerre-Gauss LG_0^3 pump with three units of angular momentum. At the position of the transmission peak at $\Delta\omega_p/\omega \approx 1.0297$, the overlap between the three-photon amplitude and the one quasi-hole wave function has the excellent value of

98.9%. The Berry phase calculated from the frequency shift $\Delta\omega_o$ of the peak via (13) is $\approx 0.163\pi$. This value is very close to the analytical prediction $\approx 0.160\pi$ obtained from the analytical form of the one quasi-hole wave function, Eq. (3) of the main text, in the three-photon case. This suggests that our scheme to measure the many-body braiding phase can successfully extend to states with a larger number of particles.

[1] In order to automatically find the coefficient of each term in a multivariate polynomial in an unexpanded form like the Laughlin wave function, we made use of the numerical package NAClab developed by Prof. Zhonggang Zeng of Northeastern Illinois University, Department of Mathematics.

[2] D. Arovas, J. R. Schrieffer, and F. Wilczek, Phys. Rev. Lett. **53**, 722 (1984).

[3] D. Yoshioka, *The Quantum Hall Effect* (Springer-Verlag, Berlin, 2002).